Supplementary Online Materials (SOM) for:

Title:

Seasonal cycles of fluorescent biological aerosol particles in boreal and semi-arid forests of Finland and Colorado

Authors:

C. J. Schumacher[1], C. Pöhlker[2], P. Aalto[3], V. Hiltunen[3], T. Petäjä[3], M. Kulmala[3], U. Pöschl[2], J. A. Huffman[1,2*]

[1]Department of Chemistry and Biochemistry, University of Denver, Denver, Colorado, USA.
[2]Department of Biogeochemistry and Multiphase Chemistry, Max Planck Institute for Chemistry, Mainz, Germany.
[3]Department of Physics, University of Helsinki, Helsinki, Finland.

*Corresponding author: alex.huffman@du.edu

Supplemental Text

S1.1 Diurnal Patterns

At the Finland site the minimum FBAP concentration occurred between 9:00 – 12:00 local time (LT) during spring through fall and was shifted a few hours earlier in winter (Fig. S3). During winter, however, the concentration of particles was significantly lower and so counting statistics were poor and average curves are noisy. The diurnal pattern of RH is smoother in each case than particle concentration and follows generally similar patterns of high values at night and lower values during the day. The timing of the RH and $N_{F,c}$ peaks are not always aligned, however, and the $N_{F,c}$ peak usually precedes the RH peak by several hours. The diurnal temperature cycle is inversely correlated to RH in all cases, the minima of which shifts later in the day during fall and winter (~7:00) as compared to spring and summer (~4:00). Figure S3 shows the 3 µm mode was very narrow and predominant during spring, summer, and fall. During the winter, however, the peaks of the diurnal size distributions shift to 1.5 µm at all hours of the day, with broader tail to both larger and smaller size. Figure S3d shows non-zero average particle concentration in sizes < 1 µm for all hours of the day, which was not the case for other seasons of the year, as was discussed in relation to the average size distribution (Fig. 3).

Diurnal trends for FBAP at the Colorado site are broadly similar to those at the Finland site, but show less consistency in particle size and average timing of peaks. The diurnal pattern for summer and fall (Figs. S4b-c) show very similar patterns to each other. The concentration is lowest at 10:00, increases until 15:00, remains stable for several hours and eventually reaches a daily maximum ~20:00. During the spring (Figure S4a), however, $N_{F,c}$ peaks in the early morning (3:00) and decrease to a minimum in the late morning (10:00). A sharp peak at 12:00 is the result of the last few days of the season in June. As was the case for the Finland site, the wintertime diurnal averages (Figure S4d) are noisy, reflecting low particle concentrations. The average diurnal trend of $N_{F,c}$ is similar to other seasons, however, peaking in the evening and lowest in the middle of the day. Whereas the diurnal size distributions at the Finland site showed consistent peaks at 3 µm, seasonal averages for the Colorado site show multiple modes that change as a function of time of day. In each season the predominant mode peaks at ~2 µm, shifting slightly for each season. As with the pattern of $N_{F,c}$, the diurnal pattern of size distributions are very similar for summer and fall. Each season shows a broad mode peaking at 2.5 µm in size, but spanning ~2-4 µm and peaking at 20:00 in time. As the concentration decreases through the night the smaller particles disappear, leaving a narrower mode at 4 µm. The diurnal pattern in the spring is different from the trend later in the year, however, with two distinct modes at 2 and 5 µm, each narrower than the modes observed during summer and fall. Also unique is the fact that the predominant mode at 2 µm is somewhat smaller in particle size than the mode during summer and fall and that the mode peaks early in the morning (3:00)

instead of late evening. The 2 μm mode then decreases in concentration, not returning until early evening. The 5 μm mode, however, begins earlier in the afternoon and remains more constant throughout the day. The diurnal pattern in winter exhibits two similar modes at 2 and 6 μm, but average concentrations are so low that they appear above the baseline (0.01 cm^{-3}) occasionally (Fig. S4d). Also important to note is that Figures S3-S4 show particle size distributions and concentrations averaged over entire seasons, and so only broad themes are visible here. Many individual modes (e.g. Fig. 3-4) appear for short periods of time and are thus not reflected in this format.

S1.2 Precipitation Effects

At the Colorado site, no precipitation was observed or recorded early on 26 July, 2011. Figure S7b1 shows the N_F size distribution in the hours before rain began to fall, during the morning when the FBAP concentration is usually low. The distribution is relatively broad, peaking at ~3 μm, and the integrated $N_{F,c}$ is 0.02 cm^{-3}. Immediately upon rain arrival, however, (Fig. S7a, red trace; 11:45) $N_{F,c}$ increases to 0.49 cm^{-3} and the size distribution becomes dominated by a narrower 2.05 μm mode (Fig. S7b2). In this case, as was common throughout the summer, the FBAP number increases with each individual rain event, even if separated only by a few minutes.

For FBAP data at the Colorado site we separated the data into three periods and calculated diurnal averages for each set independently. During periods without rain influence (Fig. S8c), FBAP concentration peaked at 3.65 μm in the late evening (20:00 – 01:00), and remains relatively unchanged in particle size throughout the day. During rain events, however, the particle size peaks at 2.5 μm at 14:00, with a secondary peak at 17:00. Further, periods with after-rain influence still show the 2.5 μm peak remaining at 14:00 and through the afternoon, though in lower concentration, but also show the 4.5 μm mode stable from midnight and into the mid-morning. Periods with rain and after-rain influence were fewer than those of no rain influence, when looked at on a seasonal basis, and so averaging statistics (Figs. S8b,c) are poorer and traces are noisier. Other seasons at the Colorado site showed a similar pattern of FBAP relationship with rain, but the correlation was much weaker (Table 1).

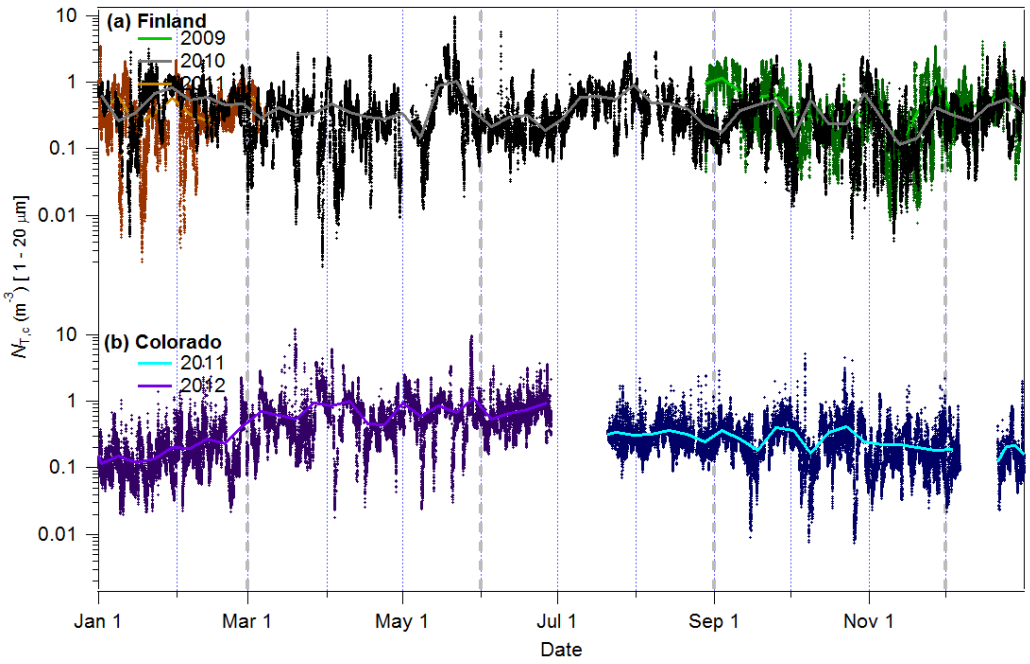

Figure S1: Overview of total particle concentration at each site. Small dots represent individual 5-minute data points from UV-APS. Colored traces cutting through UV-APS data show 7-day mean values of FBAP concentration, plotted on left axes. Axis ranges matched in upper and bottom panels. Dashed vertical lines show seasonal boundaries used for averaging (as discussed in Section 2.4).

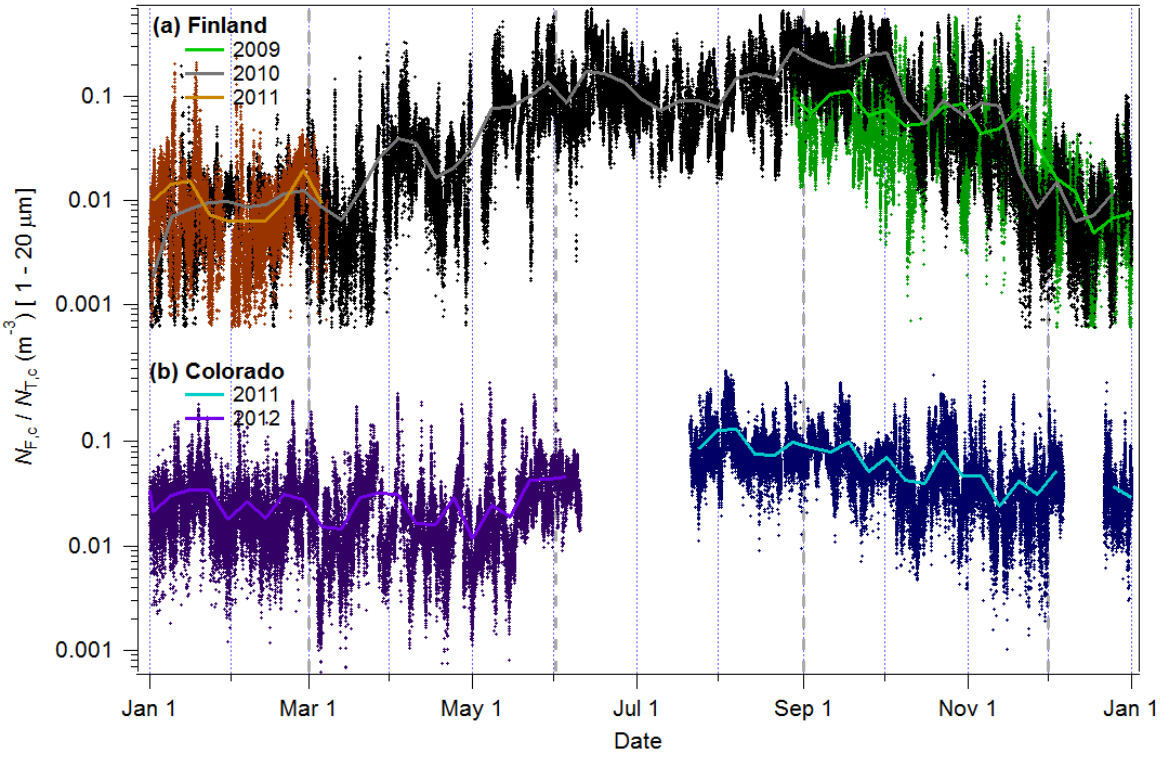

Figure S2: Overview of FBAP/total particle concentration ratio at each site. Small dots represent individual 5-minute data points from UV-APS. Colored traces cutting through UV-APS data show 7-day mean values of FBAP concentration, plotted on left axes. Axis ranges matched in upper and bottom panels. Dashed vertical lines show seasonal boundaries used for averaging (as discussed in Section 2.4)

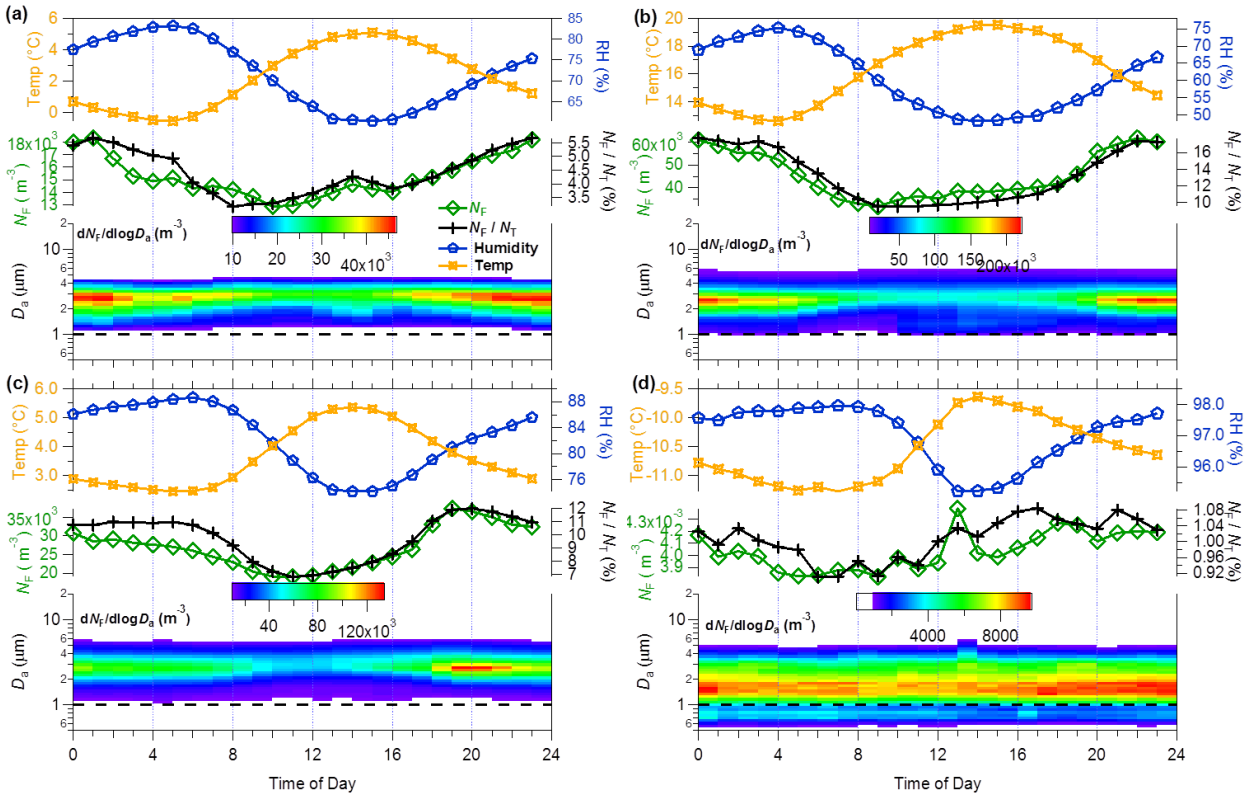

Figure S3: Seasonal diurnals trends at Finland site. FBAP concentration (green), ratio of FBAP to total particle concentration (black), temperature (yellow), and relative humidity (blue) plotted for each season: **(a)** spring **(b)** summer **(c)** fall **(d)** winter.

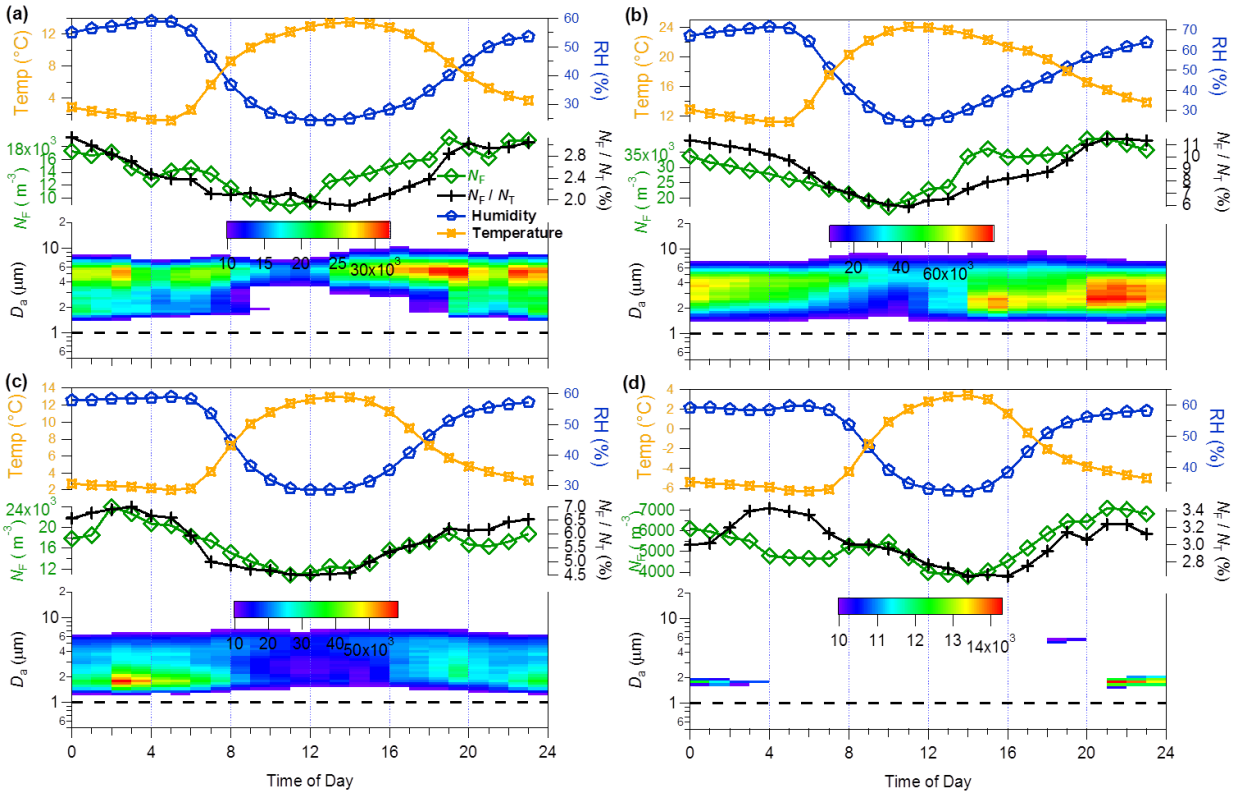

Figure S4: Seasonal diurnals trends at Colorado site. FBAP concentration (green), ratio of FBAP to total particle concentration (black), temperature (yellow), and relative humidity (blue) plotted for each season: **(a)** spring **(b)** summer **(c)** fall **(d)** winter.

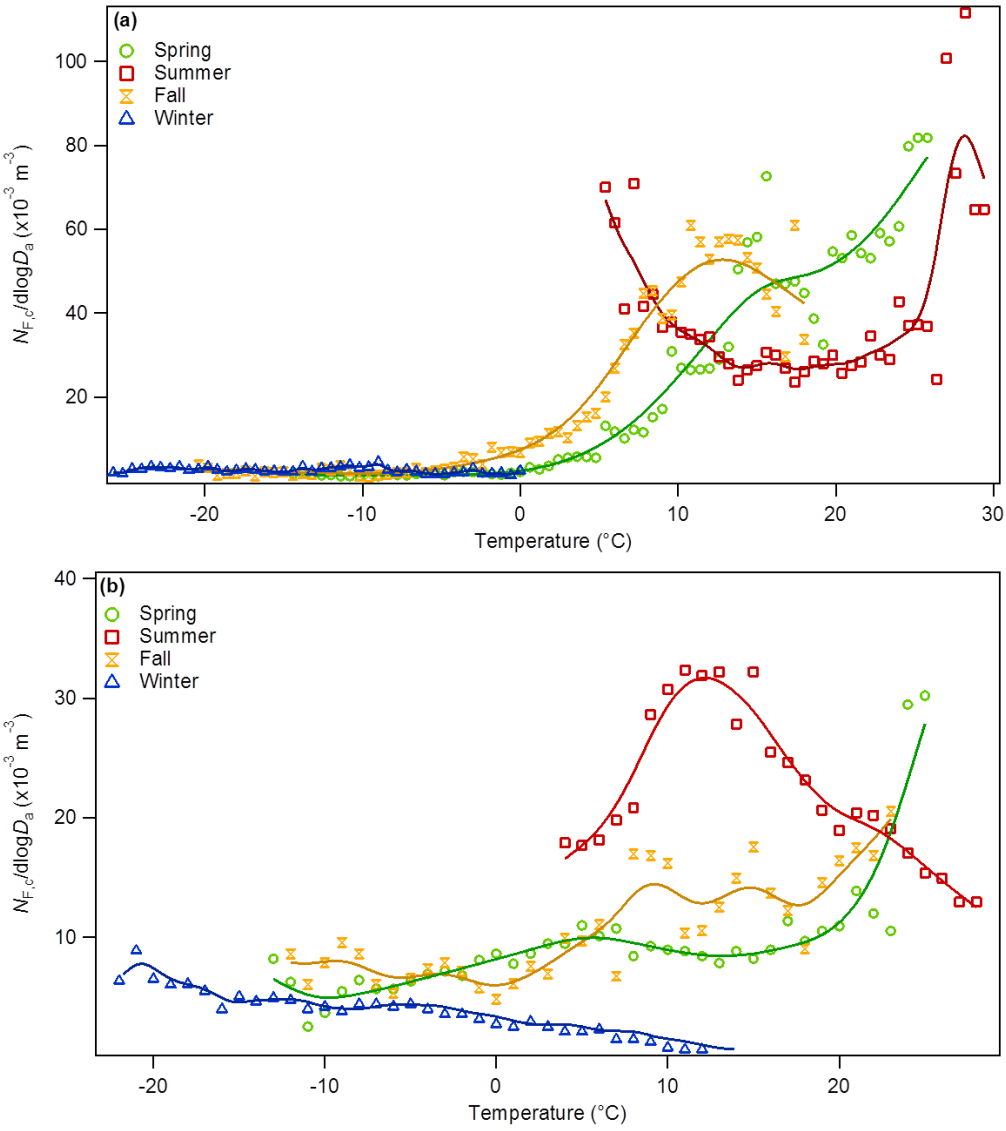

Figure S5: Median seasonal relationship between FBAP concentration and temperature. Data averaged into 100 bins. Bins that contained less than 0.01% of the total points were removed. **(a)** Finland **(b)** Colorado. Fit lines are spline curves to guide the eye.

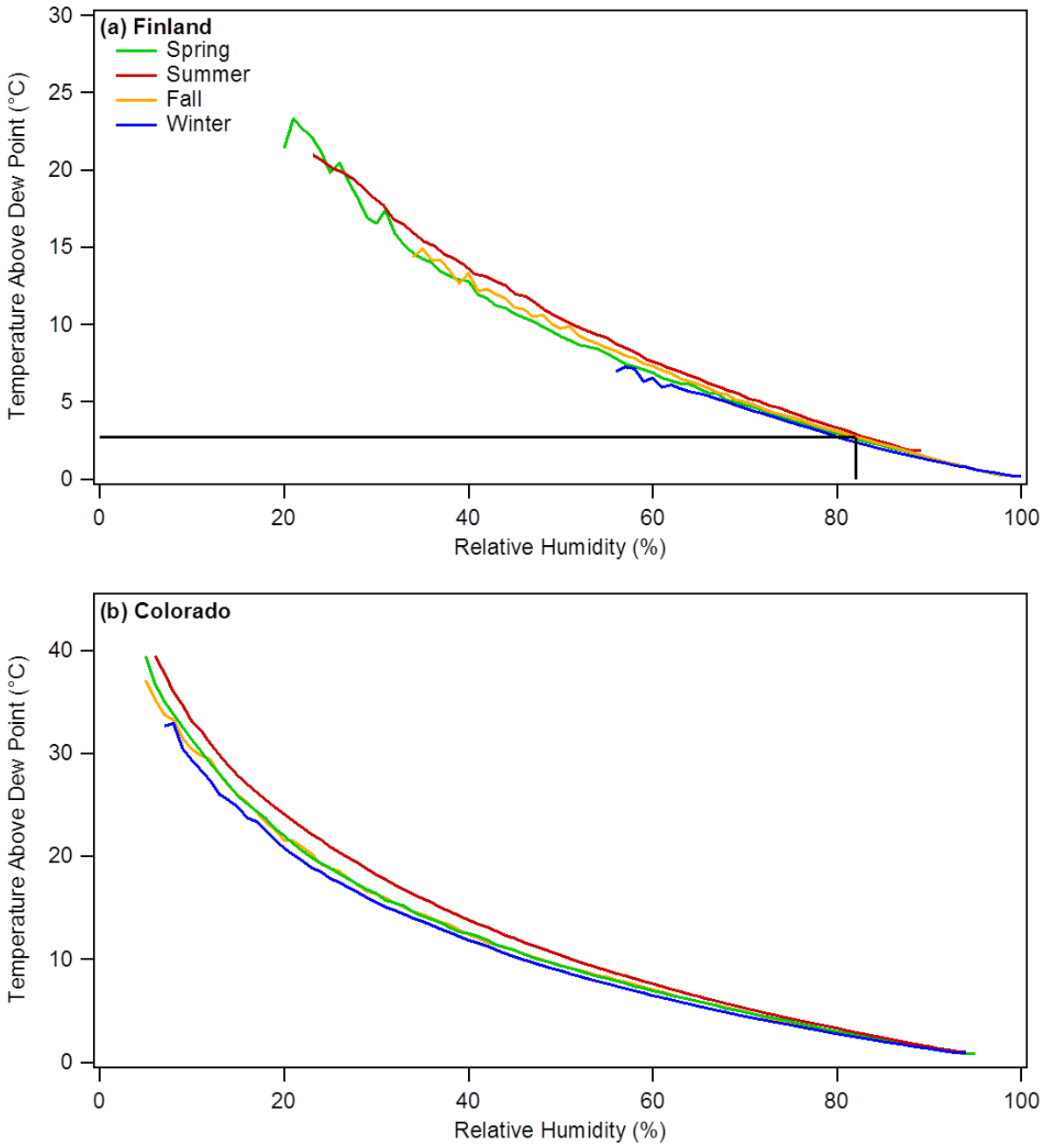

Figure S6: Relationship between RH and temperature above dew point. Gray line in each figure indicates the point at which the FBAP concentration drops drastically (Fig. 6). The following equation was used to calculate the temperature above dew point: $(\gamma_m(T, RH) = \ln(\frac{RH}{100}\exp((b - \frac{T}{d})(\frac{T}{c+T})))$; $T_{dp} = \frac{c\gamma_m(T,RH)}{b-\gamma_m(T,RH)}$; $where\ a = 6.1121, b = 18.564, c = 255.57, d = 254.4$).

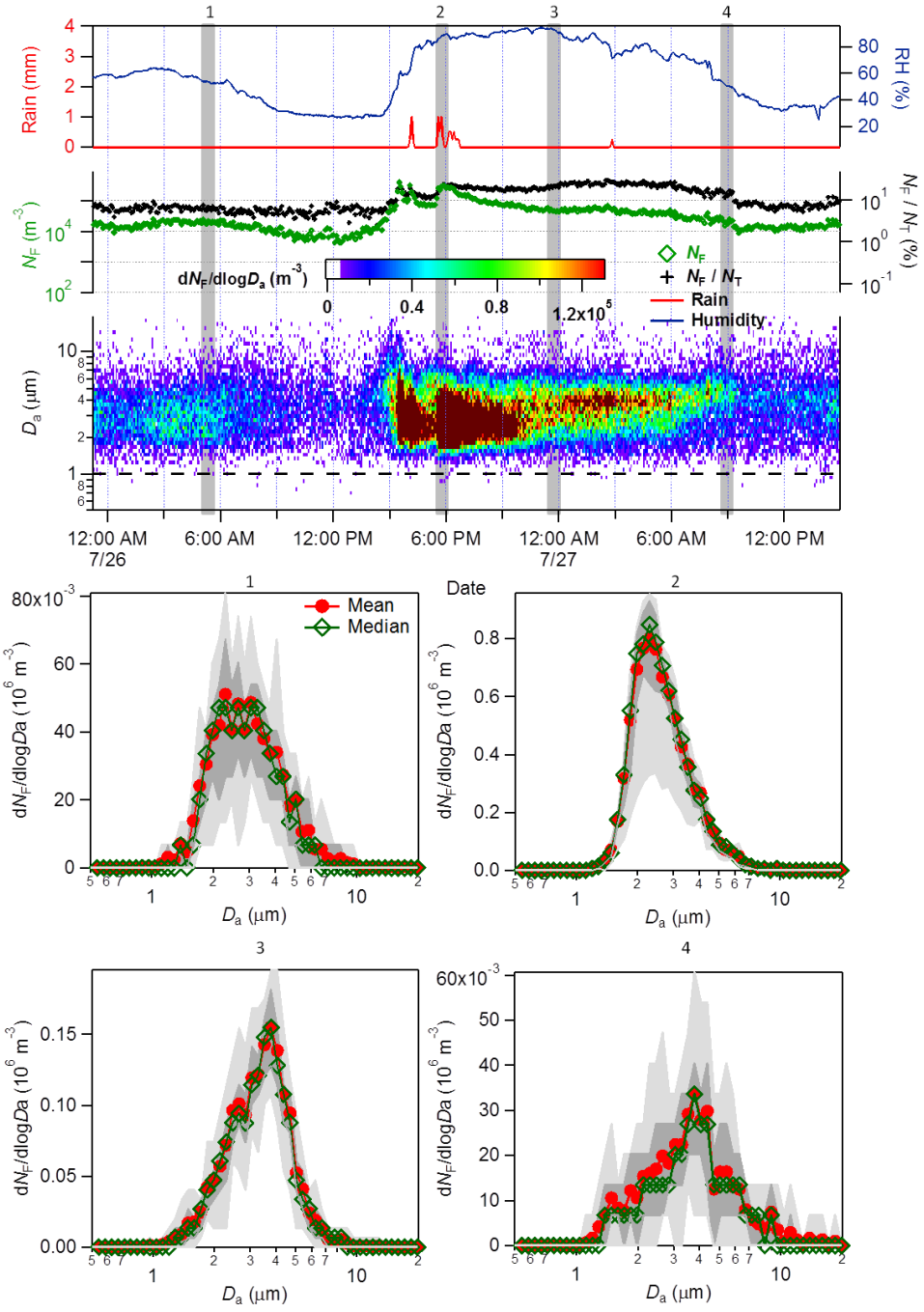

Figure S7: Example of rain influence on particle size and concentration at Colorado site. **(a)** Time series of rain, RH, FBAP, FBAP to total particle ratio, and FBAP size distributions. Numbered gray bars correlate to size distributions below. **(b)** Size distributions from periods (1) before rain, (2) during rain, (3) immediately after rain, and (4) after all rain, after-rain influence.

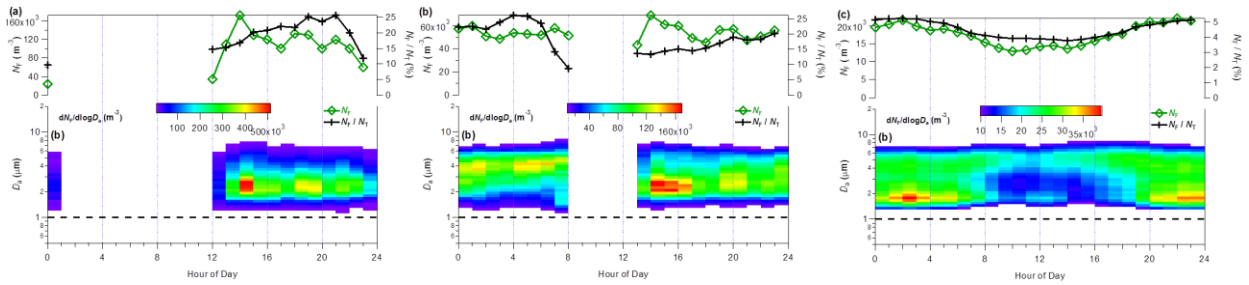

Figure S8: Diurnal averages of FBAP concentration and size distributions at Colorado site during summer separated into periods: **(a)** during rain, **(b)** immediately after rain, and **(c)** without rain influence. Averages shown here only for periods with > 8 data points.

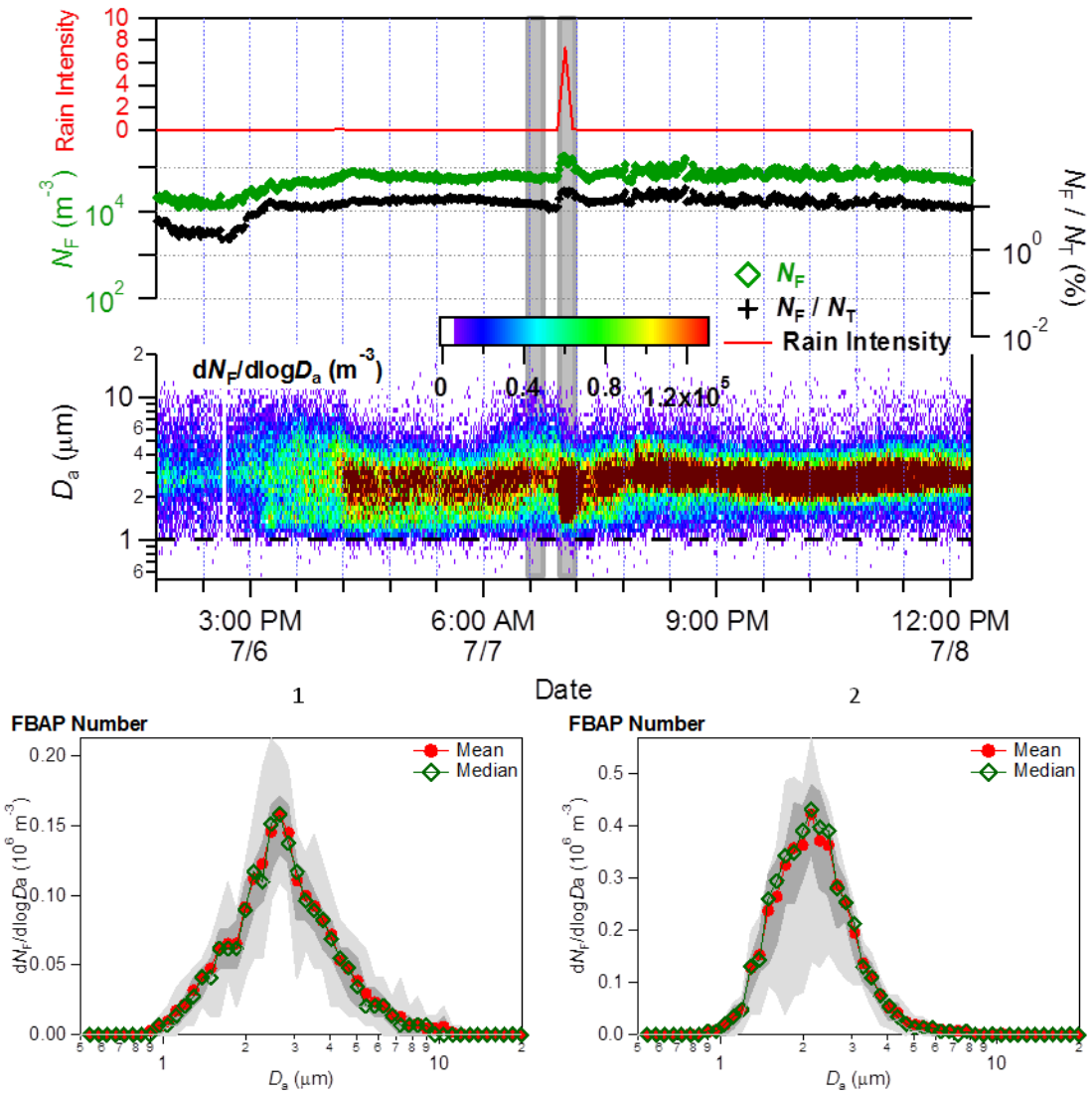

Figure S9: Example of rain influence on particle size and concentration at Finland site. **(a)** Time series of rain, RH, FBAP, FBAP to total particle ratio, and FBAP size distributions. Numbered gray bars correlate to size distributions below. **(b)** Size distributions from periods (1) before rain and (2) during rain.